Conquering poor resolution in fast magic angle spinning solid-state NMR spectra of non-crystallisable protein assemblies

30th June 2017

Ruben Tomás

Trent Franks, Peter Gierth and Józef Lewandowski

Word Count: 2194

Executive summary

- This study aimed to develop a technique to tackle inhomogeneous broadening, a major cause in the loss of site-specific information in solid-state NMR, using a technique termed saturation exchange spectroscopy (SEXY).

- Proof-of-concept was obtained using N-formyl-Met-Leu-Phe-OH (MLF), a simple tripeptide, whereby sites on the amino acid residues were selectively saturated and saturation transfer was observed.

- Optimisation of the method was achieved by investigating various parameters including nutation frequency and applied pulse saturation time. A nutation frequency of 65 Hz and saturation time of 0.300 s were deemed sufficient.

- Two-dimensional ^{13}C SEXY spectra obtained at fast and slow magic angle spinning frequencies were comparable to 2D ^{13}C-^{13}C Proton-driven spin diffusion (PDSD) spectra suggesting that SEXY was well optimised and could also be used for structural assignment.

- T_1 relaxation studies indicate the possibility of using SEXY to work towards a full relaxation matrix of MLF in future work and provide a method to determine spin diffusion rates.

- Analysis of complex inhomogeneous systems yielded no results due to hardware issues. Directing future studies on the analysis of such systems would determine if SEXY is a suitable approach for tackling inhomogeneous broadening.

Introduction

Solid-state nuclear magnetic resonance (ssNMR) is an increasingly prevalent tool providing information on the structure and dynamics of biomolecules inaccessible to solution NMR or crystallography.[1–5] However, spectral resolution can limit the amount of site-specific information extractable from NMR spectra.[6] Crystalline protein samples offer exceptional resolution; however, a large portion of biomolecules do not easily crystallise. Sedimentation and precipitation, although suitable alternative sample preparation methods, can lead to inhomogeneous broadening.[7] Such broadening effects result from the presence of a molecule in different conformations or non-uniform packing, as seen in amyloid fibrils,[8–10] which resonate at slightly different frequencies (Fig. 1).

This study aimed to devise a novel approach, saturation exchange spectroscopy (SEXY), to tackle poor resolution by selectively saturating peaks, as explained in Fig. 1. Firstly, a simple crystalline model system, N-formyl-Met-Leu-Phe-OH (MLF), characterised by limited inhomogeneous broadening was required to provide proof-of-concept and to optimise the method. Application of this approach on samples containing varying degrees of inhomogeneous broadening, including the B1 domain of protein G (GB1) and an amyloid-β fibril (Aβ1-42), was subsequently attempted.
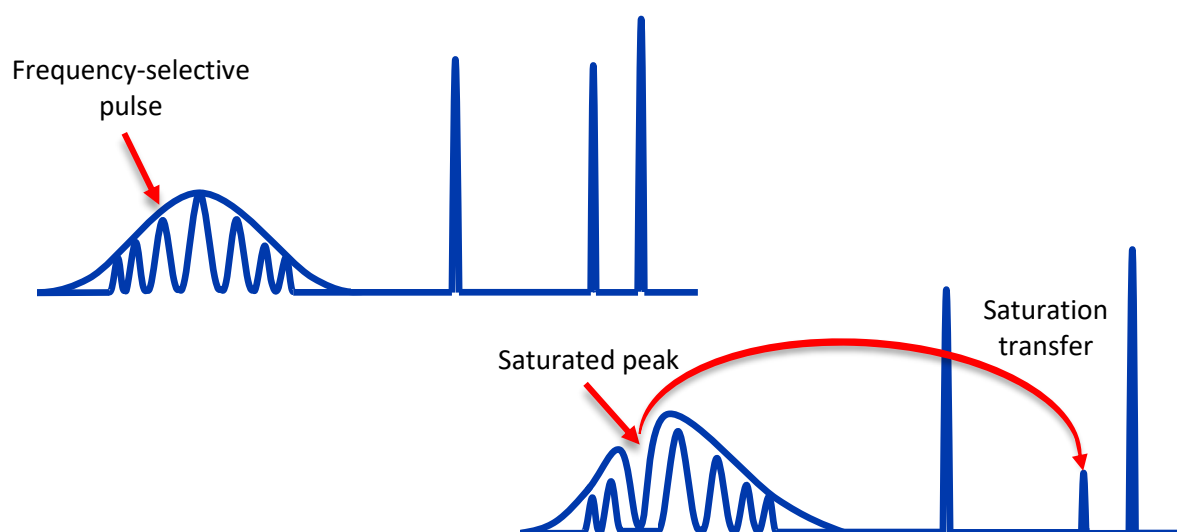

Figure 1. Saturation exchange spectroscopy's application in inhomogeneous broadening. NMR requires the absorbance of RF radiation to cause 'flipping' of nuclear spins between two spin states (in the case of ^{13}C) with a population imbalance. Frequency-selective RF pulses, of sufficiently high energy, irradiate single peaks within a broadened region resulting in equalisation of populations within both spin states. Thus, the NMR signal sharply decreases (saturates). Saturation transfer subsequently occurs *via* spin diffusion, a process driven by dipolar coupling (through space interactions), resulting in the loss of signal of coupled peaks. Spin diffusion arises among nuclear spins of the same kind (like-spins) within a few to several Angstroms in space.[11] Therefore, previously unattainable structural information, from broadened peaks, is now accessible. Spin diffusion occurs due to the presence of $I_i^+I_j^-$ and $I_iI_j^+$ terms within the dipolar spin Hamiltonian between two like-spins.[11,12] These terms cause mutual flipping of two nearby spins resulting in a transfer of polarisation from the first spin to the second. This mechanism causes propagation of spin polarisation until it is lost by longitudinal relaxation (T_1) processes.

Results and Discussion

Analysis of MLF

Proof-of-concept

MLF (Fig. 3) was selected to test selective saturation using the pulse sequence developed, as described in Fig. S1 (supplementary information), and to determine the extent of saturation transfer. Firstly, a 1D ^{13}C spectrum of MLF (Fig. 2) was obtained to provide the RF pulse frequencies necessary for the SEXY experiments. Previous literature[13,14] was used to assign the spectrum and the results are illustrated in Table 1.
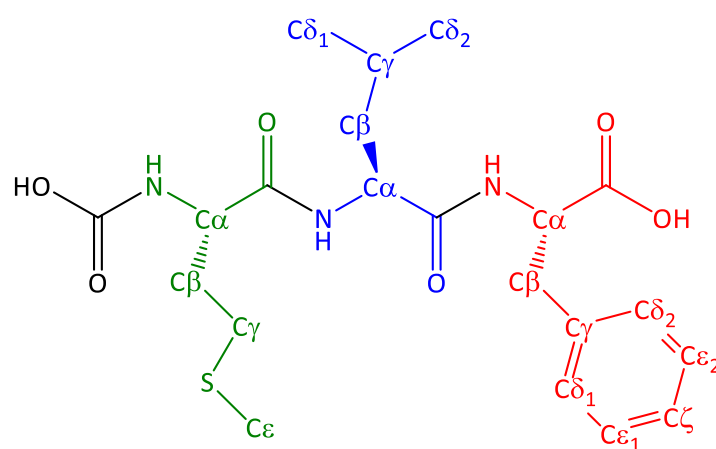
Figure 2. Chemical structure of MLF. The simple tripeptide consists of methionine (green), leucine (blue) and phenylalanine-OH (red) residues.
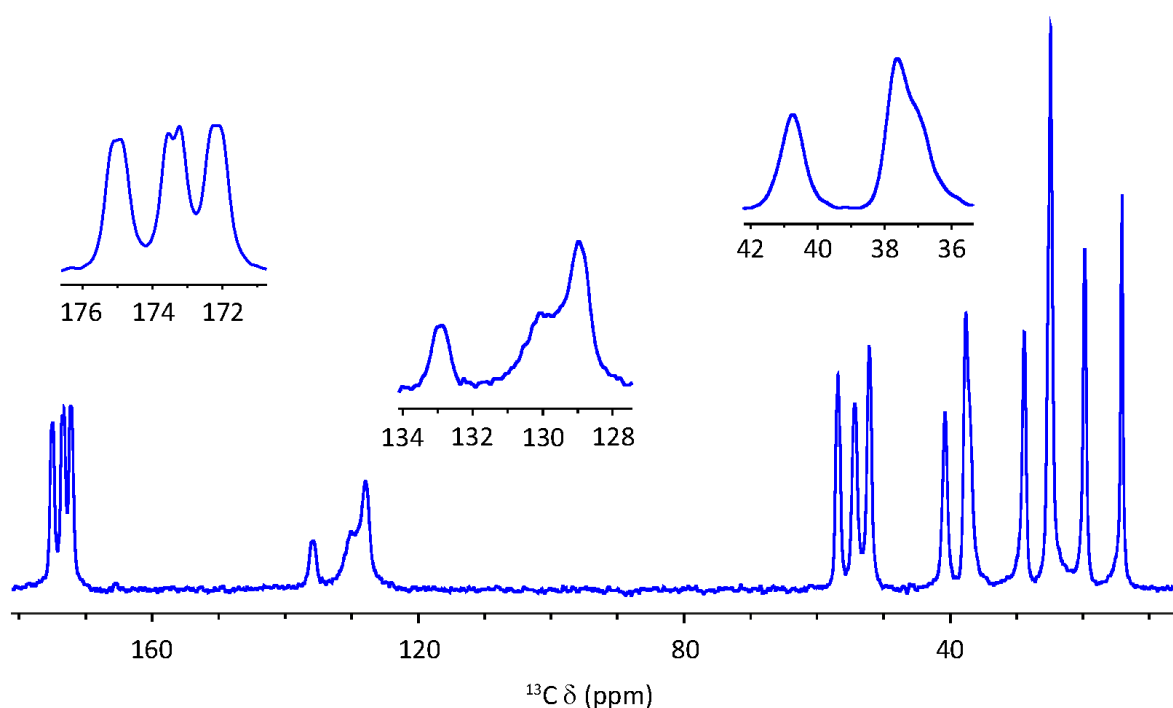
Figure 3. One-dimensional ^{13}C-spectrum of MLF. The frequencies of each peaks were noted and utilised for subsequent selective saturation using weak RF pulses.

Table 1. MLF ^{13}C 1D chemical shift assignments.

| Amino acid residue	Chemical shift (ppm)						
	C′	C$^\alpha$	C$^\beta$	C$^\gamma$	C$^\delta$	C$^\varepsilon$	C$^\zeta$
Methionine	172.2	52.1	37.6[a]	28.8	-	14.1	-
Leucine	175.0	56.8	40.7	24.9	19.7	-	-
Phenolphthalein	173.5	54.3	37.2[a]	135.7		127.9[b]	

[a] Peaks for the C$^\beta$ of methionine and phenolphthalein were not completely resolved. [b] Unambiguous assignment of the aromatic peaks of phenolphthalein was unsuccessful due to unresolved peaks, so the chemical shift provided is of the most intense and upfield peak.

A preliminary 2D ^{13}C SEXY experiment was conducted to determine if saturating peaks and saturation transfer were attainable. The 2D spectrum obtained (Fig. 5a) was different from a 'typical' 2D experiment. Instead, the indirect dimension corresponded to RF pulses applied at selected frequencies, with each frequency corresponding to a specific site of the amino acid residue. For simplicity, the indirect dimension was labelled pulse numbers. In Fig. 5a, direct saturation of sites and saturation transfer resulted in the formation of a 'hole', or attenuation in the intensity of the peaks, providing a good indication that the pulse sequence developed was successful. Nevertheless, visualisation of changes in peak intensity in this manner was difficult, leading to extensive loss of information.
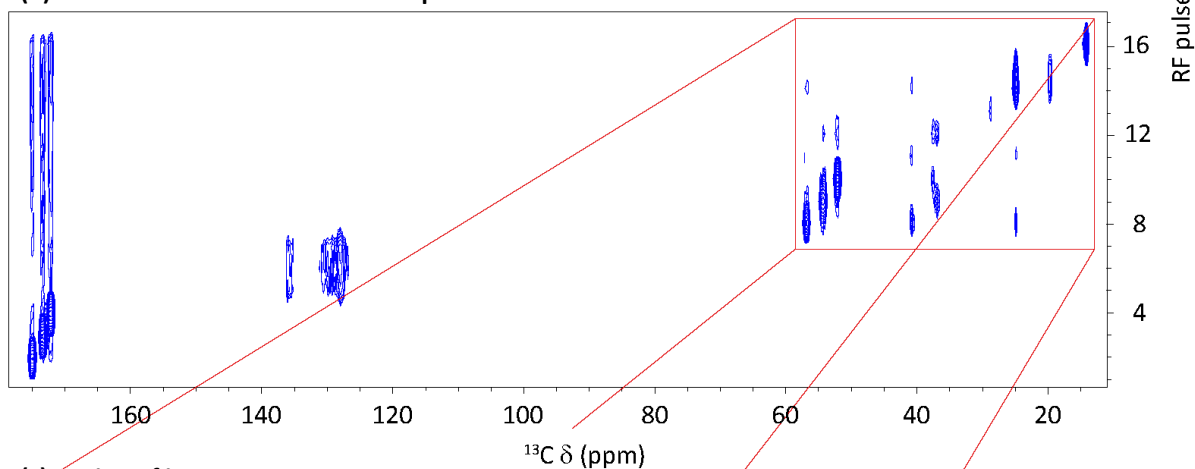
A difference spectrum (Fig. 5b) was obtained by subtracting each row of the original spectrum (Fig. 5a) with an unsaturated 1D spectrum, to produce the final 2D ^{13}C SEXY spectrum. Any 'hole' or attenuation in peak intensity was now clearly visible as peaks, similar to a conventional 2D spectrum. This method of spectral reconstruction allowed correlations due to saturation transfer to be clearly identified, potentially allowing structural determination of larger peptides. All subsequent spectra were processed in this manner. Each row possessed one peak with a chemical shift equal to the frequency of the applied RF pulse, this was the directly saturated site. All additional peaks were due to saturation transfer, a process limited by distance. Therefore, peak correlations were expected of proximal atoms.

Saturation of the carbonyl groups produced a single peak in each row, at the frequency of the applied pulse. However, no saturation transfer peaks were visible with proximal atoms, suggesting the absence of spin diffusion. Similarly, selective saturation within the aromatic region revealed saturation transfer only between carbons within the aromatic structure. The rate of spin diffusion is largely dependent on dipolar coupling. Although the use of cross-polarisation (CP) increased the rate of spin diffusion, owing to the high gamma-ratio of protons producing a strong network of dipolar coupling, it was reduced by

(a) Original 2D ¹³C SEXY spectrum
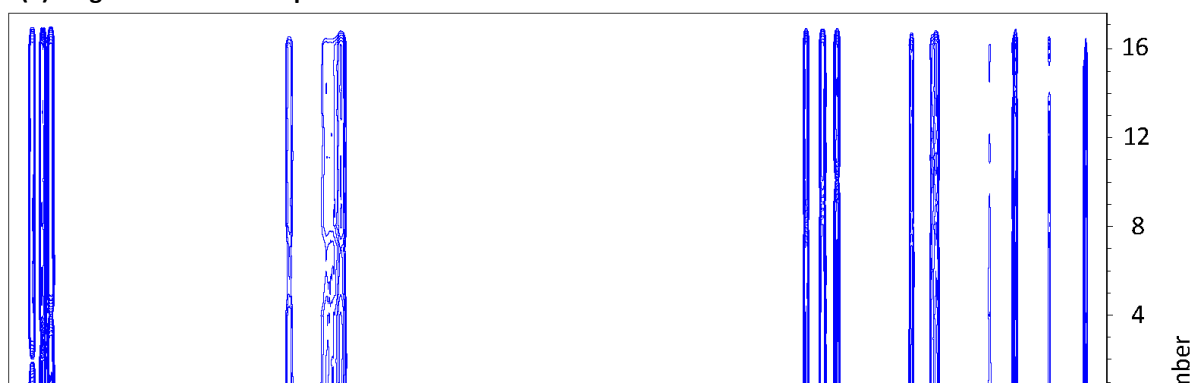
(b) Final reconstructed 2D ¹³C SEXY spectrum

(c) Region of interest
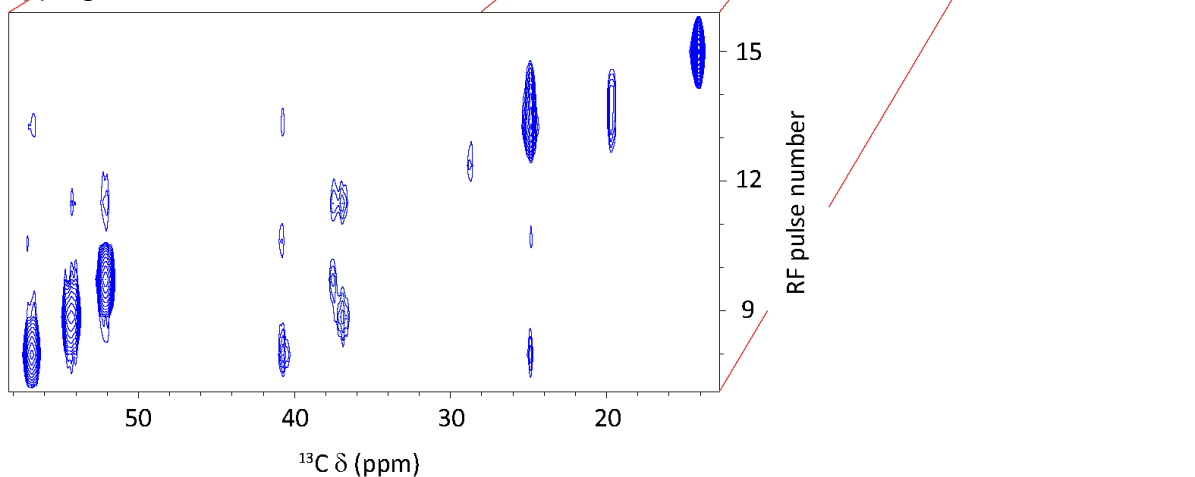
Figure 4. Two-dimensional ¹³C SEXY spectra of fMLF. Each row in the indirect dimension of the spectra consists of a saturation pulse at a specific frequency. (b) An easy to interpret difference spectrum was obtained by subtracting each row of (a) the original data by a 1D unsaturated spectrum. (c) The aliphatic region was of most interest as extensive saturation transfer is visible. In total, 17 saturation pulses were applied, two of which were off-resonance, at the following frequencies (ppm): 188.9 (1), 174.8, 173.2, 172.0, 135.6, 130.0, 127.8, 56.8, 54.3, 52.1, 40.6, 37.6, 28.8, 24.8, 19.7, 14.1 and -9.9 (17).

MAS.[15] The lack of saturation transfer suggested that the MAS spinning frequency used was sufficient enough to average the dipolar coupling between the carbonyl and aromatic groups with all other atoms

to the lowest order, and thus also spin diffusion. For this reason, saturation of the aromatic carbons was avoided in future experiments.

The aliphatic region (Fig. 5c) presented a more extensive network of spin diffusion, which has been summarised in Table 2. Direct saturation at the C^α frequencies yielded saturation transfer peaks of greatest intensity. As previously mentioned, spin diffusion occurs until polarisation is lost by T_1 relaxation processes. In this study, longitudinal relaxation determined the length of time required for the equally populated spin states, to return to Boltzmann's equilibrium. Therefore, the C^α groups most likely possess slower T_1 relaxation rates allowing a longer time for saturation transfer to occur.

Saturation of methionine's C^β produced saturation transfer peaks to the phenolphthalein amino acid residue. MLF's tertiary structure[13,18] suggests that if saturation transfer was possible in this manner then further transfer should have been observed with closer atoms. Therefore, as the chemical shifts of methionine's and phenolphthalein's C^β were similar, it is likely that both were saturated simultaneously with pulse 13.

Table 2. Summary of results for the aliphatic region of interest (Fig. 5c).[a]

RF pulse number	Saturation frequency (ppm)	Directly saturated	Saturation transfer
9	56.8	C^α (Leu)	C^β (Leu) C^γ (Leu)
10	54.3	C^α (Phe)	C^β (Phe)
11	52.1	C^α (Met)	C^β (Met)
12	40.7	C^β (Leu)	C^α (Leu) C^γ (Leu)
13	37.6	C^β (Met)[b]	C^α (Phe), C^α (Met), C^β (Phe)
14	28.8	C^γ (Met)	-
15	24.9	C^γ (Leu)	C^α (Leu), C^β (Leu), C^δ (Leu)
16	19.7	C^δ (Leu)	C^γ (Leu)
17	14.1	C^ε (Met)[c]	-

[a] Direct saturation of phenolphthalein's C^β was mistakenly not completed. [b] Direct saturation of methionine's C^β led to simultaneous indirect saturation of phenolphthalein's C^β. [c] Saturation of methionine's C^ε yielded no transfer peaks as it is isolated by the presence of sulphur.

The 'streaks' observed in the carbonyl region were likely artefacts introduced by the reconstruction method used. Alternatively, a low signal-to-noise ratio (SNR) could have been responsible due to the low number of scans completed.

Optimisation

The ability to selectively saturate one peak, resulting in the attenuation of another peak is very powerful, providing a suitable approach to tackle inhomogeneous broadening. The previous results demonstrated the ability for saturation transfer to occur over 1 or 2 bonds, potentially also providing a novel experiment for sidechain assignment of amino acid residues. However, spin diffusion is known to transfer saturation efficiently, especially in techniques such as saturation transfer difference.[19,20] Thus, optimisation of the method was required to determine if saturation transfer could be increased, initially without decreasing the MAS spinning frequency. Firstly, the nutation frequency of the saturation pulse was investigated to alter the pulse width and power to avoid simultaneous saturation of peaks. Secondly, the duration of saturation was altered to investigate its influence on saturation transfer.

Three-dimensional ^{13}C SEXY spectra were recorded using nutation frequencies of 65 Hz, 200 Hz and 500 Hz and processed as before. The second indirect dimension (F1) consisted of ten different saturation times ranging from 0.01 s to 16.00 s. Two-dimensional slices were acquired at 3 saturation times, 0.03 s, 0.30 s and 3.00 s (Fig. 6). Simultaneous saturation of proximal peaks was obtained by increasing the saturation pulse width and power, as expected. A nutation frequency of 65 Hz was deemed sufficient for the completion of this study. However, inhomogeneous systems require lower nutation frequencies to selectively saturate regions within broadened peaks. Unfortunately, due to hardware limitations (preamplifier and voltage gating systems), 65 Hz was the smallest nutation frequency possible with a 600 MHz spectrometer. To achieve saturation transfer at lower nutation frequencies longer irradiation is required, as seen in Fig. 6, increasing the overall analysis time. Alternatively, narrower Gaussian pulses could be used, instead of square. The optimum saturation time was 0.30 s at a nutation frequency of 65 Hz, displaying minimal 'streaks'.

Increasing saturation time and nutation frequency produced 'streaks' from oversaturation and unexpected peaks at off-resonance frequencies (pulse 1 and 15). These unanticipated peaks were likely caused by sample heating, despite the use of weak saturation pulses. A second possibility considered was the observation of chemical shift anisotropy (CSA). MAS averages out these anisotropic interactions, leaving behind mainly isotropic interactions. However, saturation of residual CSA *via* off-resonance pulses could have resulted in saturation transfer.

Variable temperature control and a presaturation step were used in subsequent experiments to ensure that the temperature remained consistent prior to acquisition.
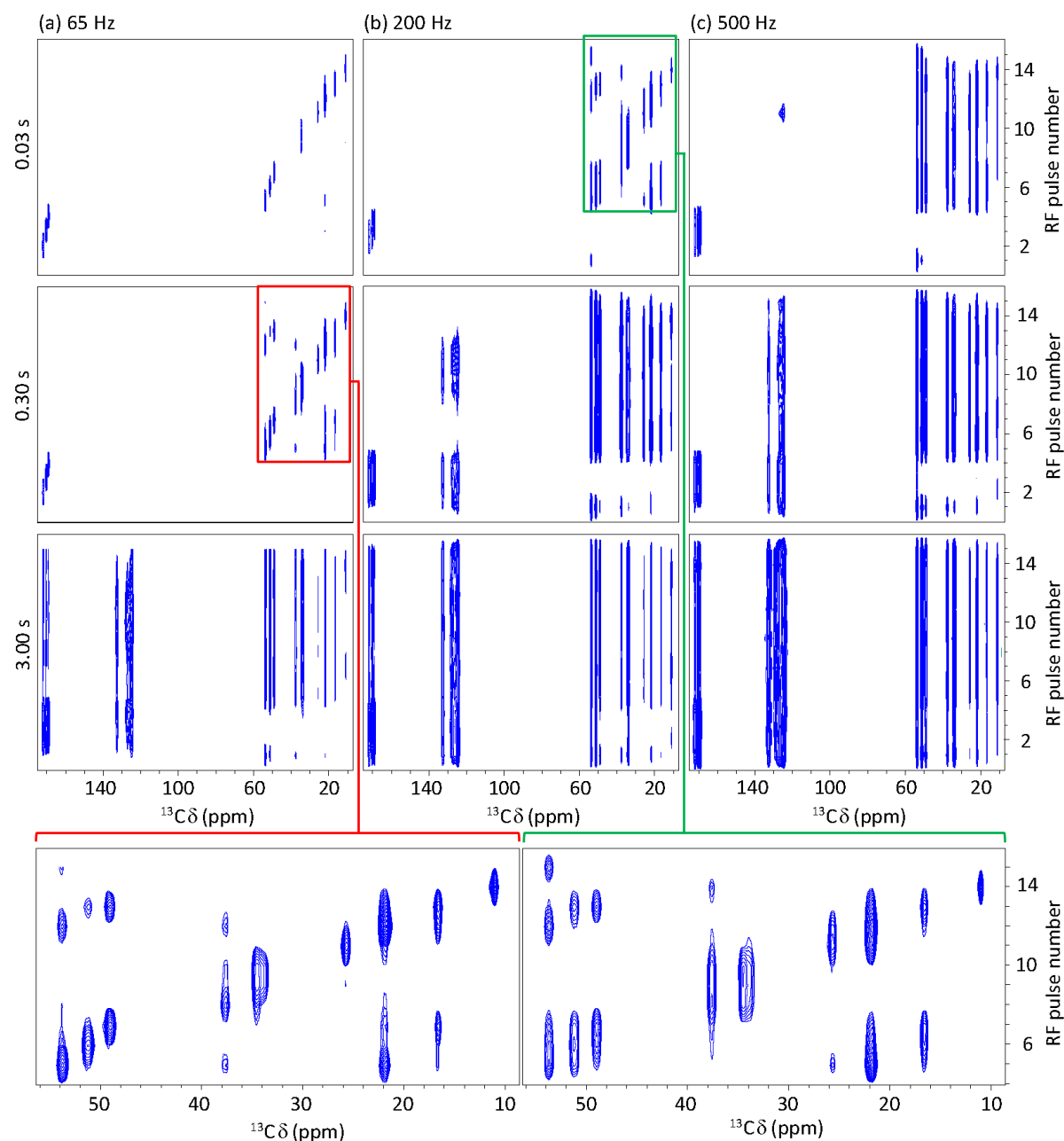
Figure 5. Two-dimensional slices removed from three 3D ^{13}C SEXY experiment obtained at different nutation frequencies and saturation durations. The nutation frequencies used were (a) 65 Hz, (b) 200 Hz and (c) 500 Hz. The additional indirect dimension (F1) corresponded to changes in saturation duration. Ten saturation times were used; however, slices of the 3D spectrum were taken at saturation times of 0.03 s, 0.30 s and 3.00 s. In total, 15 saturation pulses were applied, two of which were off-resonance, at the following frequencies (ppm): 222.0 (1), 174.8, 173.2, 172.0, 56.8, 54.3, 52.1, 40.6, 37.5, 36.9, 28.8, 24.8, 19.7, 14.1 and -43.0 (15).

Chemical shift anisotropy

Mapping of chemical shift anisotropy was attempted using a 'grid search' method. Saturation pulses were applied within a large frequency interval at increments of 250 Hz. The 2D ^{13}C SEXY spectrum obtained (Fig. 6a) did not resemble a CSA pattern. Instead, the appearance of artefacts was observed due to a fault in the pulse sequence developed. Initially, the saturation pulse used alternated between phase X and Y, introducing periodicity, which was thought to increase saturation efficiency. However, as the two phases are not completely symmetrical, artefacts were introduced.
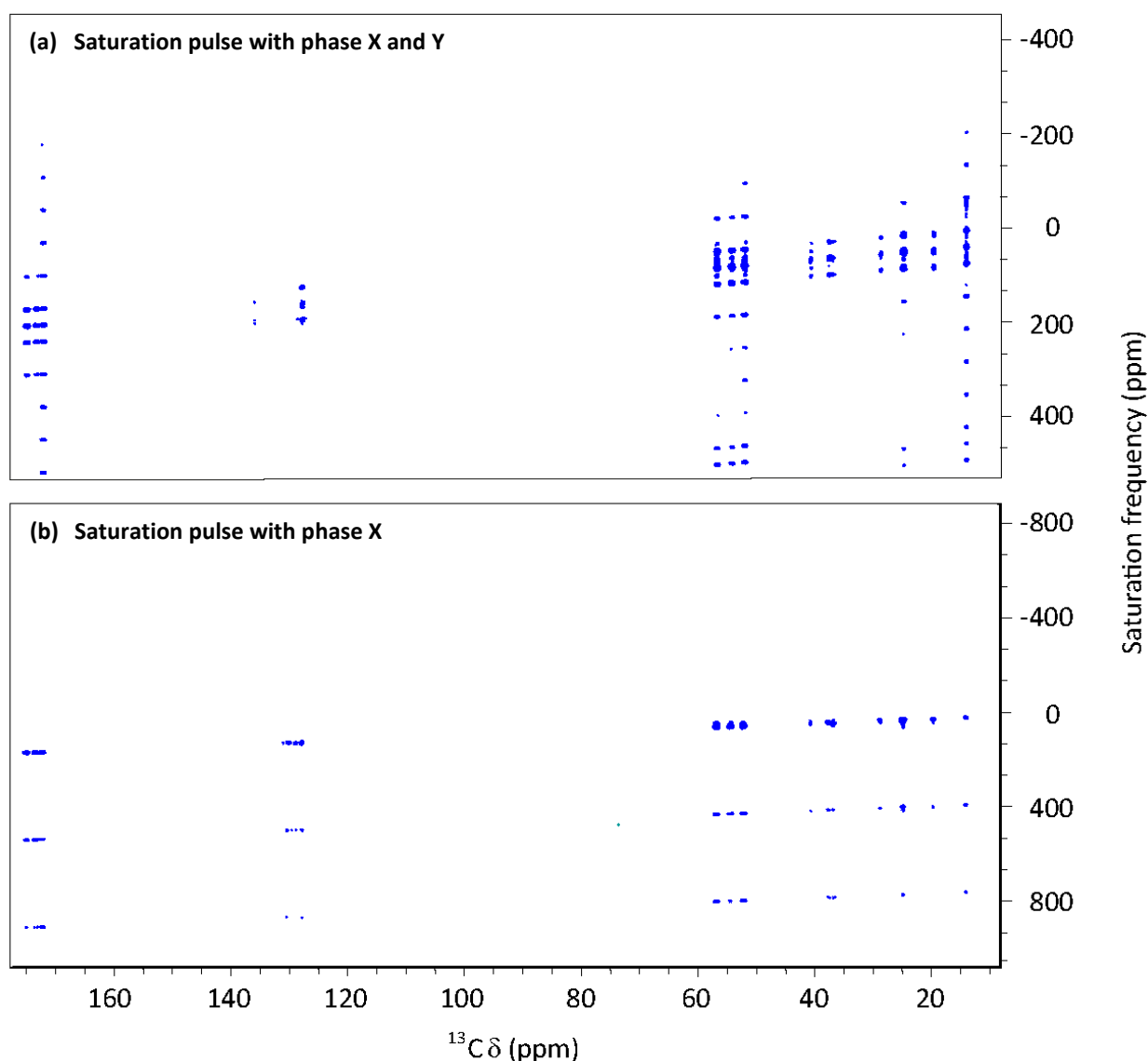
Figure 6. Mapping of chemical shift anisotropy using a 'grid search' method. Two 2D ^{13}C SEXY spectra were obtained with (a) a saturation pulse alternating between phase X and Y and (b) a saturation pulse with only phase X. Saturation was completed between large intervals, with saturation pulse frequencies increasing in 250 Hz (~1.6 ppm) increments. Utilising a saturation pulse with phase X revealed spinning sidebands at 60 kHz apart. Lower frequency side bands were not visible due to insufficient number of scans.

A 'grid search' spectrum was subsequently acquired using a saturation pulse with only phase X, removing all artefacts and revealing only spinning side bands at 60 kHz apart (Fig. 6b). Therefore, subsequent experiments were conducted with saturation pulses with phase X.

Comparison of SEXY with PDSD

Proton-driven spin diffusion (PDSD) also relies on spin diffusion for the transfer of polarisation between spins. PDSD's pulse sequence is similar to that of SEXY, with the only differences being the presence of T_1 evolution and mixing time and absence of frequency-selective saturation RF pulses.[21,22] Therefore, a SEXY spectrum was expected to possess cross peaks analogous to those obtained in PDSD. The successfulness of the optimised SEXY experiment was investigated by comparing a 2D ^{13}C SEXY spectrum with a 2D ^{13}C-^{13}C PDSD spectrum (Fig. 8) obtained using the same saturation/ mixing time (0.3 s).

The entire PDSD spectrum has been provided in the supplementary information (Fig. S3), however no saturation transfer was exhibited from saturating the carbonyl groups. In addition, the aromatic region
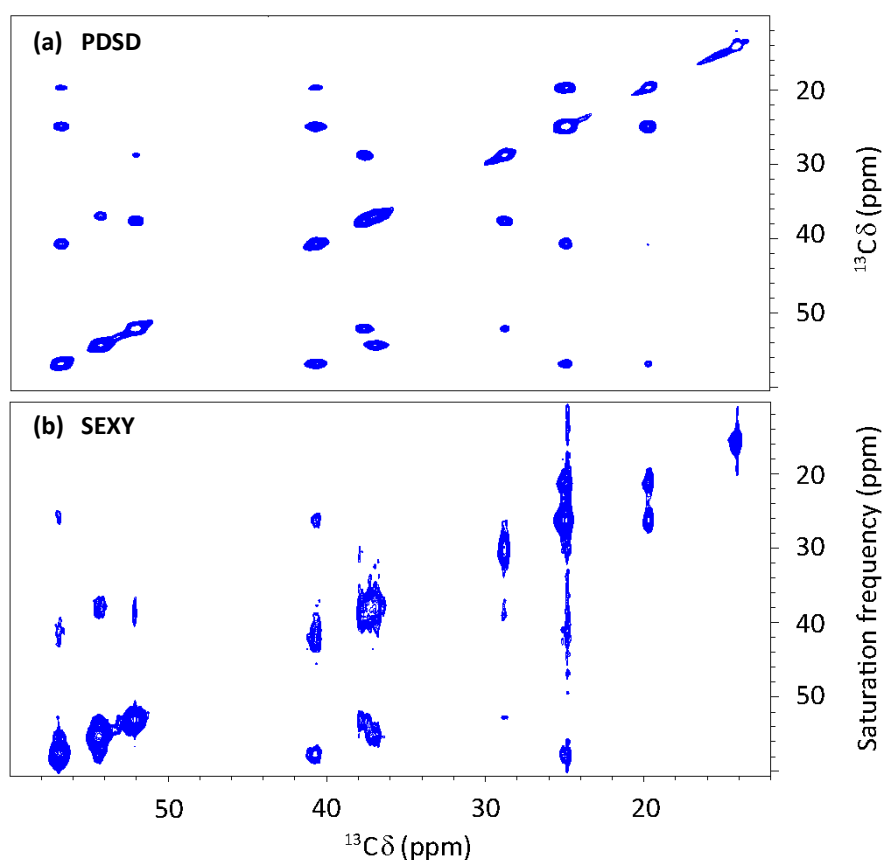
Figure 8. Two-dimensional ^{13}C spectra obtained using (a) PDSD and (b) SEXY. A mixing/ saturation time of 0.300 s was utilised. The total analysis time for the PDSD experiment was ~3.5 hours and ~1.5 hours for the SEXY experiment.

only demonstrated saturation transfer between carbons within the aromatic ring. These results were consistent with those obtained during the proof-of-concept experiment. Peak correlations within the aliphatic region of both spectra, which contained extensive saturation transfer, were compared and documented in Table 3.

SEXY and PDSD produced comparable spectra, with SEXY possessing fewer cross peaks. Low intensity cross peaks were only visible in the PDSD spectrum, indicating that optimisation of SEXY was required to increase sensitivity. Nevertheless, the absence of T_1 evolution and mixing times in SEXY reduced the duration of the experiment from ~3.5 hours in PDSD to ~ 1.5 hours. To produce spherical peaks in the SEXY spectrum, saturation pulses surrounding the desired frequencies were introduced. This contributed to an increase in the analysis time, which could be avoided. However, the spectrum was made more analogous to a conventional PDSD spectrum. The remaining streaks were

Table 3. Comparison of results obtained from the PDSD and SEXY spectra (Fig. 8)

Chemical Shift (ppm)	Directly saturated/ site of interest	PDSD cross peaks	SEXY cross peaks
56.8	C^α (Leu)	C^β (Leu), C^γ (Leu), C^δ (Leu)	C^β (Leu), C^γ (Leu)
54.3	C^α (Phe)	C^β (Phe)	C^β (Phe)
52.1	C^α (Met)	C^β (Met), C^γ (Met)	C^β (Met), C^γ (Met)
40.7	C^β (Leu)	C^α (Leu), C^γ (Leu), C^δ (Leu)	C^α (Leu), C^γ (Leu),
37.6	C^β (Met)	C^α (Met), C^γ (Met)	C^α (Met), C^γ (Met)
36.8	C^β (Phe)	C^α (Phe)	C^α (Phe)
28.8	C^γ (Met)	C^α (Met), C^β (Met)	-
24.9	C^γ (Leu)	C^α (Leu), C^β (Leu), C^δ (Leu)	C^α (Leu), C^β (Leu), C^δ (Leu)
19.7	C^δ (Leu)	C^α (Leu), C^β (Leu), C^γ (Leu)	C^γ (Leu)[a]
14.1	C^ϵ (Met)	-	-

[a] *The main difference between PDSD and SEXY was the lack of cross peaks present when leucine's C^δ was directly saturated.*

likely a combination of low SNR and artefacts introduced from spectral reconstruction. Low sensitivity was an issue with SEXY, as there were no evolution and mixing times. Therefore, fast analysis time was obtained at the expense of sensitivity, a concern as NMR is already an intrinsically insensitive technique.

Decreasing MAS spinning frequency

To study the effects of spin diffusion on the appearance of a SEXY spectrum, the MAS spinning frequency was reduced to 13.3 kHz to increase spin diffusion. Previous PDSD studies using a MAS spinning frequency of 7 kHz and mixing time of 0.3 s revealed cross peaks between all atoms of all residues.[21] Thus, it was unsurprising that the SEXY spectrum obtained under similar conditions (Fig. 9) possessed peaks visualised as 'streaks'. Complete transfer of saturation between all site of MLF, including the carbonyl and aromatic groups, were visible at a saturation time of 0.3 s. Complex inhomogeneous systems contain extensive dipolar networks, so this could be problematic. Applying saturation pulses above and below the desired frequencies may resolve this issue, hopefully producing spherical peaks.
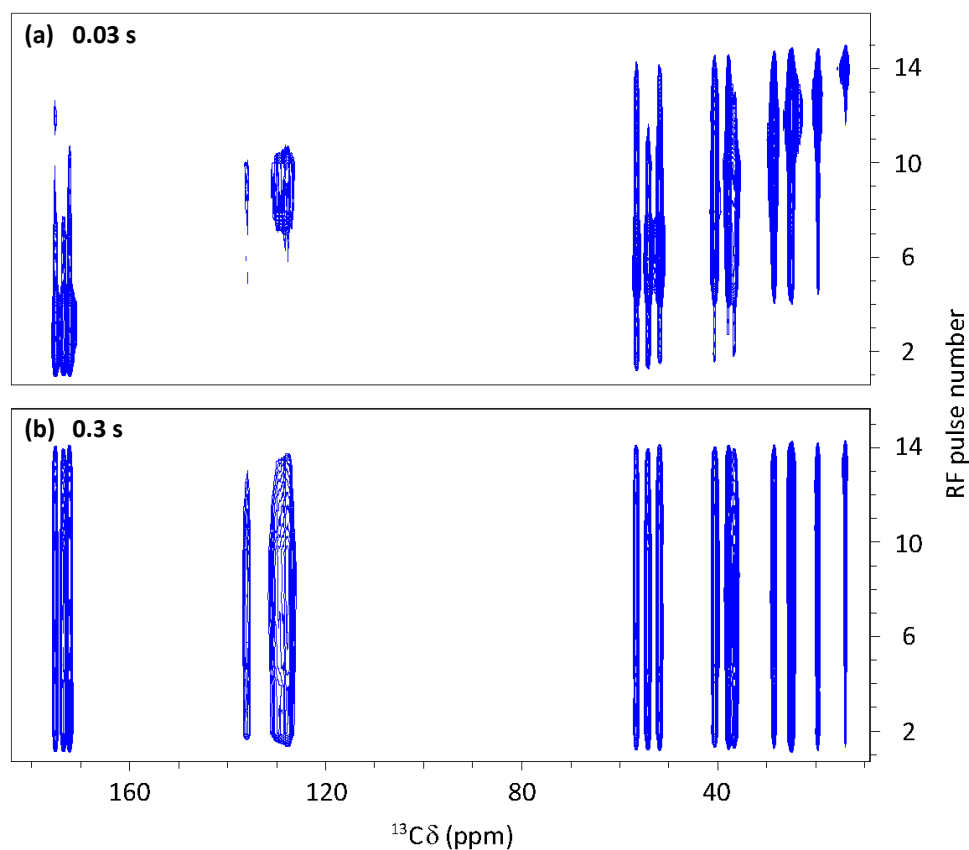
Figure 7. Two-dimensional ^{13}C SEXY spectra of fMLF obtained at MAS spinning frequencies of 13.3 kHz and saturation times of (a) 0.03 s and (b) 0.3 s.

T_1 relaxation studies

T_1 relaxation studies were conducted as a measure of working towards a full relaxation matrix of MLF. T_1 relaxation data was acquired from a 3D ^{13}C SEXY spectrum with different pulse saturation times as the second indirect dimension. Normalised T_1 relaxation measurements (Table S1 and S2) were used to construct a scatterplot resembling a conventional 2D spectrum (Fig. 10). Frequency-selective saturation caused a sharp drop in T_1 relaxation times. The increased spin diffusion at a spinning frequency of 13.3 kHz resulted in visible drops in the T_1 relaxation times of other residue sites due to saturation
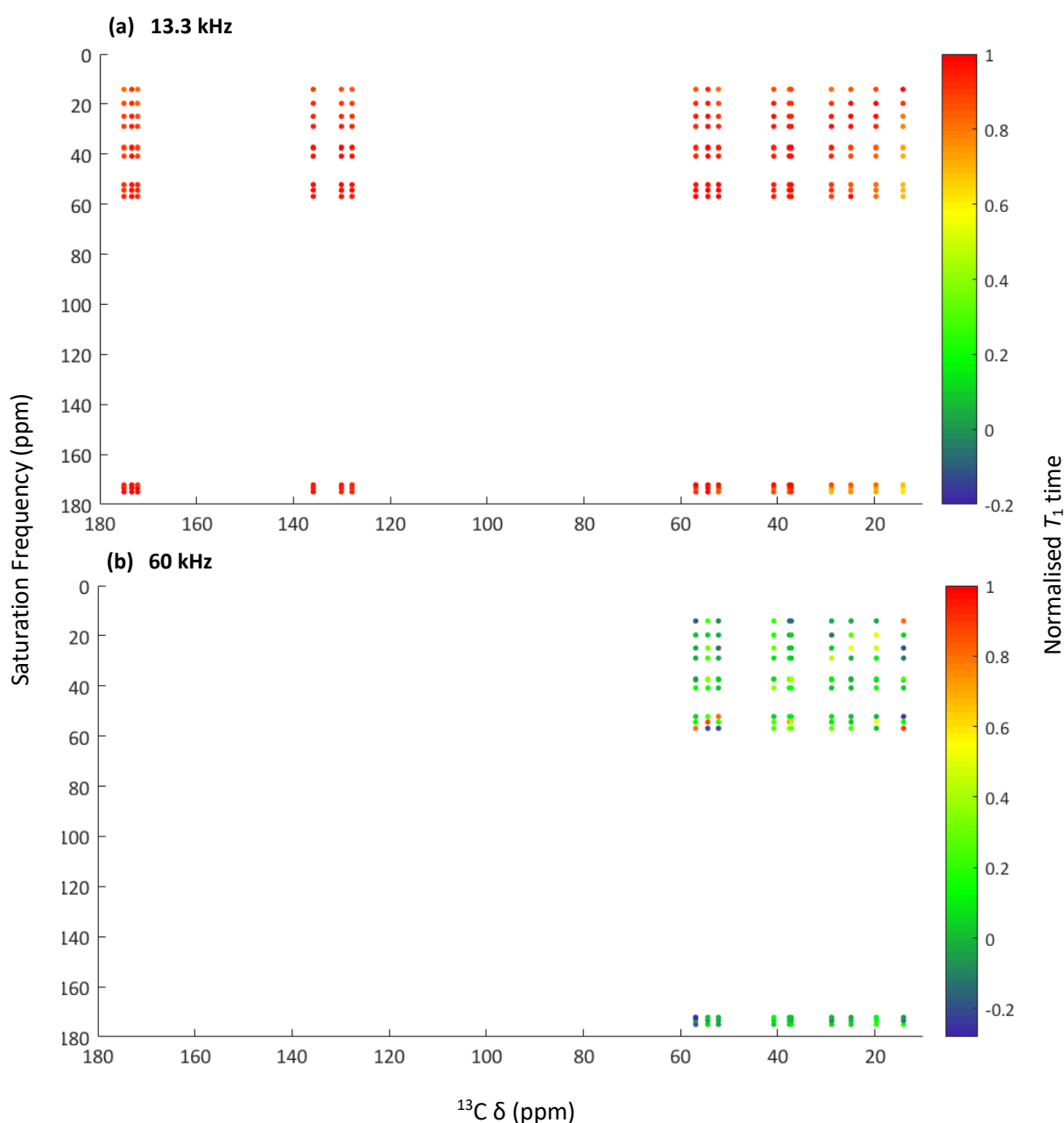
Figure 8. Normalised T1 relaxation time scatterplot resembling a 2D ^{13}C-SEXY spectrum. Normalised T1 relaxation times below -0.2 are highlighted in Table S1 and were given a value of -0.2.

transfer, whereas only a small degree of saturation transfer was visible at the higher spinning frequency, as expected.

Acquiring T_1 relaxation values at a spinning frequency of 60 kHz presented multiple issues, including the presence of normalised T_1 times below 0. Furthermore, the carbonyl and aromatic groups possessed unsaturated T_1 relaxation times above the maximum pulse saturation time (15.00 s), so could not be obtained reliably. Reliable T_1 relaxation measurements for the carbonyl and aromatic groups were acquired at the slower spinning frequency due to faster relaxation rates from increased spin diffusion. Unfortunately, due to hardware issues, the saturation time could not be further increased. Nevertheless, these T_1 relaxation time maps provided an alternative method of 2D spectral reconstruction, removing the streaks previously observed at slow spinning frequencies (Fig. 9). Future studies could be directed in studying how T_1 relaxation times of cross peaks change depending on the saturated site as a possible approach to calculate spin diffusion rates.

Analysis of complex systems

SEXY was attempted on amyloid-β oligomers (Aβ1-42), which contain inhomogeneous broadening, and GB1 to determine if the approach is feasible for larger, more complex systems. However, due to hardware issues, including unstable spinning and incorrectly inputted power levels, no results were obtained.

Conclusion

Saturation exchange spectroscopy (SEXY) presents a rapid, novel approach with the potential to tackle inhomogeneous broadening, as well as providing a platform for structural determination, spin diffusion rate calculations and working towards a full relaxation matrix of MLF. Although future work is necessary to fully optimise this technique, results attained are comparable to those from PDSD with a ~57% reduction in analysis time. Directing future studies to the application of SEXY to complex inhomogeneous systems could provide a solution to one of ssNMR's greatest issues.

Future Work

Apply SEXY to inhomogeneous systems to determine its feasibility in tackling inhomogeneous broadening. Further optimise SEXY by decreasing the nutation frequency on a spectrometer capable of doing so, or use gaussian-shaped saturation pulses. Continue working towards a full relaxation matrix of MLF and develop a method for spin diffusion rate calculations using T_1 relaxation times.

Acknowledgments

References

1   L. K. Thompson, *Curr Opin Struc Biol*, 2002, **12**, 661–669.

2   M. J. Knight, A. J. Pell, I. Bertini, I. C. Felli, L. Gonnelli, R. Pierattelli, T. Herrmann, L. Emsley and G. Pintacuda, *Proc. Natl. Acad. Sci.*, 2012, **109**, 11095–11100.

3   A. Böckmann, *Angew. Chemie - Int. Ed.*, 2008, **47**, 6110–6113.

4   F. Castellani, B. Van Rossum, A. Diehl, M. Schubert, K. Rehbein and H. Oschkinat, *Nature*, 2002, **420**, 23–26.

5   M. Weingarth, P. Tekely, R. Brüschweiler and G. Bodenhausen, *Chem. Commun.*, 2010, **46**, 952–954.

6   S. E. Ashbrook and S. Sneddon, *J. Am. Chem. Soc.*, 2014, **136**, 15440–15456.

7   J. M. Lamley, D. Iuga, C. Öster, H. J. Sass, M. Rogowski, A. Oss, J. Past, A. Reinhold, S. Grzesiek, A. Samoson and J. R. Lewandowski, *J. Am. Chem. Soc.*, 2014, **136**, 16800–16806.

8   S. Sharpe, K. Simonetti, J. Yau and P. Walsh, *Biomacromolecules*, 2011, **12**, 1546–1555.

9   A. Reymer, K. K. Frederick, S. Rocha, T. Beke-Somfai, C. C. Kitts, S. Lindquist and B. Nordén, *Proc. Natl. Acad. Sci.*, 2014, **111**, 17158–17163.

10   A. W. P. Fitzpatrick, G. Debelouchinac, M. Bayroc, D. Clared, M. Caporinic, V. Bajajc, C. Jaroniecc and L. Wang, *Atomic structure and hierarchical assembly of a cross-β amyloid fibril*, 2013, vol. 5590.

11   K. Akasaka, in *Encyclopedia of Biophysics*, ed. G. Roberts, Springer, Heidelberg, Berlin, 1st edn., 2013, pp. 149–150.

12   M. Ernst and B. Meier, in *Solid State NMR of Polymers*, eds. I. Ando and T. Asakura, Elsevier, Amsterdam, 1st edn., 1998, pp. 83–122.

13   C. M. Rienstra, L. Tucker-Kellogg, C. P. Jaroniec, M. Hohwy, B. Reif, M. T. McMahon, B. Tidor, T. Lozano-Perez and R. G. Griffin, *Proc. Natl. Acad. Sci. U. S.*

A., 2002, **99**, 10260–10265.

14   C. M. Rienstra, M. Hohwy, M. Hong and R. G. Griffin, *J. Am. Chem. Soc.*, 2000, **122**, 10979–10990.

15   G. F. Taylor, P. Marius, C. Ford and P. T. F. Williamson, in *Handbook of Biopolymer-Based Materials*, eds. S. Thomas, D. Durand, C. Chassenieux and P. Jyotishkumar, Wiley-VCH, Weinhem, 1st edn., 2013, pp. 403–436.

16   R. Riek, G. Wider, K. Pervushin and K. Wüthrich, *Proc. Natl. Acad. Sci. U. S. A.*, 1999, **96**, 4918–4923.

17   D. Nietlispach, R. T. Clowes, R. W. Broadhurst, Y. Ito, J. Keeler, M. Kelly, J. Ashurst, H. Oschkinat, P. J. Domaille and E. D. Laue, *J. Am. Chem. Soc.*, 1996, **118**, 407–415.

18   C. P. Jaroniec, C. Filip and R. G. Griffin, *J. Am. Chem. Soc.*, 2002, **124**, 10728–10742.

19   M. Williamson, in *Annual Reports on NMR Spectroscopy, Volume 65*, ed. G. Webb, Elsevier, London, 1st edn., 2009, pp. 77–105.

20   N. Rama Krishna and V. Jayalakshmi, *Prog. Nucl. Magn. Reson. Spectrosc.*, 2006, **49**, 1–25.

21   T. Wang, J. K. Williams, K. Schmidt-Rohr and M. Hong, *J. Biomol. NMR*, 2015, **61**, 97–107.

22   M. Veshtort and R. G. Griffin, *J. Chem. Phys.*, , DOI:10.1063/1.3635374.

Supplementary Information

Experimental

All solid-state NMR spectra shown were acquired using a Bruker Avance II+ spectrometer at a [1]H Larmor frequency of 600 MHz. [U-^{13}C,^{15}N]-labelled MLF (~2.5 mg, ~5.7 μmol) was packed into a Bruker 1.3 mm triple-resonance (HXY) magic angle spinning (MAS) probe and a MAS frequency of 60 kHz was used, unless specified otherwise. Referencing was completed against alanine and SPINAL64 (15 kHz) decoupling was used throughout. All spectra were processed using TopSpin 3.5.

Proof-of-concept and Optimisation

One-dimensional ^{13}C NMR spectra were obtained using a simple ^{1}H-^{13}C cross-polarisation (CP) sequence (Fig. S1a), consisting of a hard 2.5 µs π/2 (^{1}H) pulse, CP contact time of 1 ms and 2.5 s recycle delay. The total duration of the experiment was 51 s with 16 scans completed.

Two- and three-dimensional ^{13}C SEXY spectra were acquired with a newly developed homonuclear saturation exchange sequence (Fig. S1b) consisting of a 2.5 µs π/2 (^{1}H) pulse, CP contact time of 1 ms, two 3.5 µs π/2 (^{13}C) pulses and 3.0 s recycle time. Saturation (SAT) was achieved by applying RF pulses at the frequencies obtained from the 1D ^{13}C CP/MAS spectra. In addition, three unsaturated spectra were obtained where no RF pulse was applied and two off-resonance pulses. The duration of
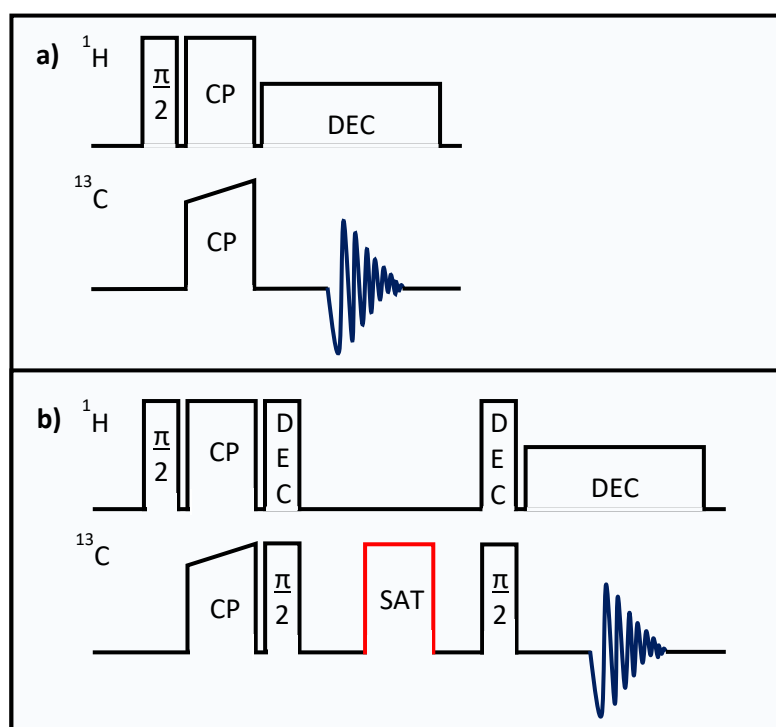
Figure S1. Schematic representation of solid-state NMR pulse sequences. (a) 1D ^{13}C-CP NMR spectra with: 2.5 s recycle delay, π/2 (^{1}H) = 2.5 µs and 1 ms CP contact time. (b) 2D and 3D ^{13}C-SEXY spectra with: 3.0 s recycle delay, π/2 (^{1}H) = 2.5 µs, 1 ms CP contact time and two π/2 (^{13}C) = 3.5 µs. Decoupling (DEC) of ^{1}H was completed.

the applied saturation pulses (saturation time), for the 3D spectra, was 0.01 s, 0.03 s, 0.10 s, 0.30 s, 1.00 s, 3.00 s, 4.50 s, 6.00 s, 8.00 s and 16.00 s. Two-dimensional spectra were obtained with a 1 s saturation time. RF pulses were investigated at three nutation frequencies, 65 Hz, 200 Hz and 500 Hz. The total duration of the 2D and 3D experiments were 28 min and 2h 38 min, with 32 and 16 scans completed, respectively.

All experiments following proof-of-concept and optimisation were obtained utilising saturation pulses with a nutation frequency of 65 Hz and temperature control. The variable temperature control system was set to 20ºC, with a gas flow pressure of 1200 l/h and probe heater set to 60 %. A 'presaturation' step was added consisting of a pulse with a duration equal to the difference between the maximum and current pulse saturation duration.

Chemical shift anisotropy

Two-dimensional ^{13}C SEXY spectra were acquired as before, however with a CP contact time of 2 ms. Initially, saturation using a pulse alternating between phase X and Y was completed between -80000 Hz and 80000 Hz, increasing in increment of 250 Hz. Saturation using a pulse with phase X was subsequently completed between 160000 Hz and -160000 Hz increasing in increments of 250. The total number of scans collected for the first and second experiment was 8 and 2, respectively. The total duration of each experiment was ~6.5 hours.

Comparison of SEXY with PDSD

A ^{13}C-PDSD spectrum was obtained with the same operating parameters as the 2D ^{13}C SEXY obtained during proof-of-concept. However, the mixing time was set to 0.3 s. A 3D ^{13}C SEXY spectrum was obtained with the indirect dimension consisting of different saturation times (0.01 s, 0.03 s, 0.10 s, 0.30 s, 1.00 s, 5.00 s, 10.00 s and 15.00 s). This spectrum was used for T_1 relaxation studies. A 2D slice was selected at a saturation time of 0.3 s for comparison with PDSD. The duration of the SEXY experiment was ~7 hours, however the slice of interest was obtained in ~1.5 hours. The duration of the PDSD experiments was ~3.5 hours and the total number of scans for both experiments was 4.

Decreasing MAS spinning frequency

A 3D ^{13}C SEXY spectrum was recorded as previously, however the MAS spinning frequency was reduced to 13.3 kHz. Furthermore, the saturation times used were 0.001 s, 0.010 s, 0.030 s, 0.100 s, 0.300 s, 1.000 s, 2.000 s and 4.000 s. The total number of scans recorded was 2 and the duration of the experiment was ~ 1.5 hours. Relaxation data was obtained from this spectrum.

Analysis of complex systems

[U-^{2}H,^{13}C,^{15}N]-labelled crystalline GB1 and [U-^{13}C,^{15}N]-labelled Aβ1-42 were packed into Bruker 1.3 mm triple-resonance (HXY) magic angle spinning (MAS) probe. Stable spinning of Aβ1-42 was unattainable. Acquisition of a 2D 13C SEXY experiment was attempted of GB1. However, no results were obtained as no saturation pulse power was inputted.

Alternative method of visualising 2D-SEXY spectrum
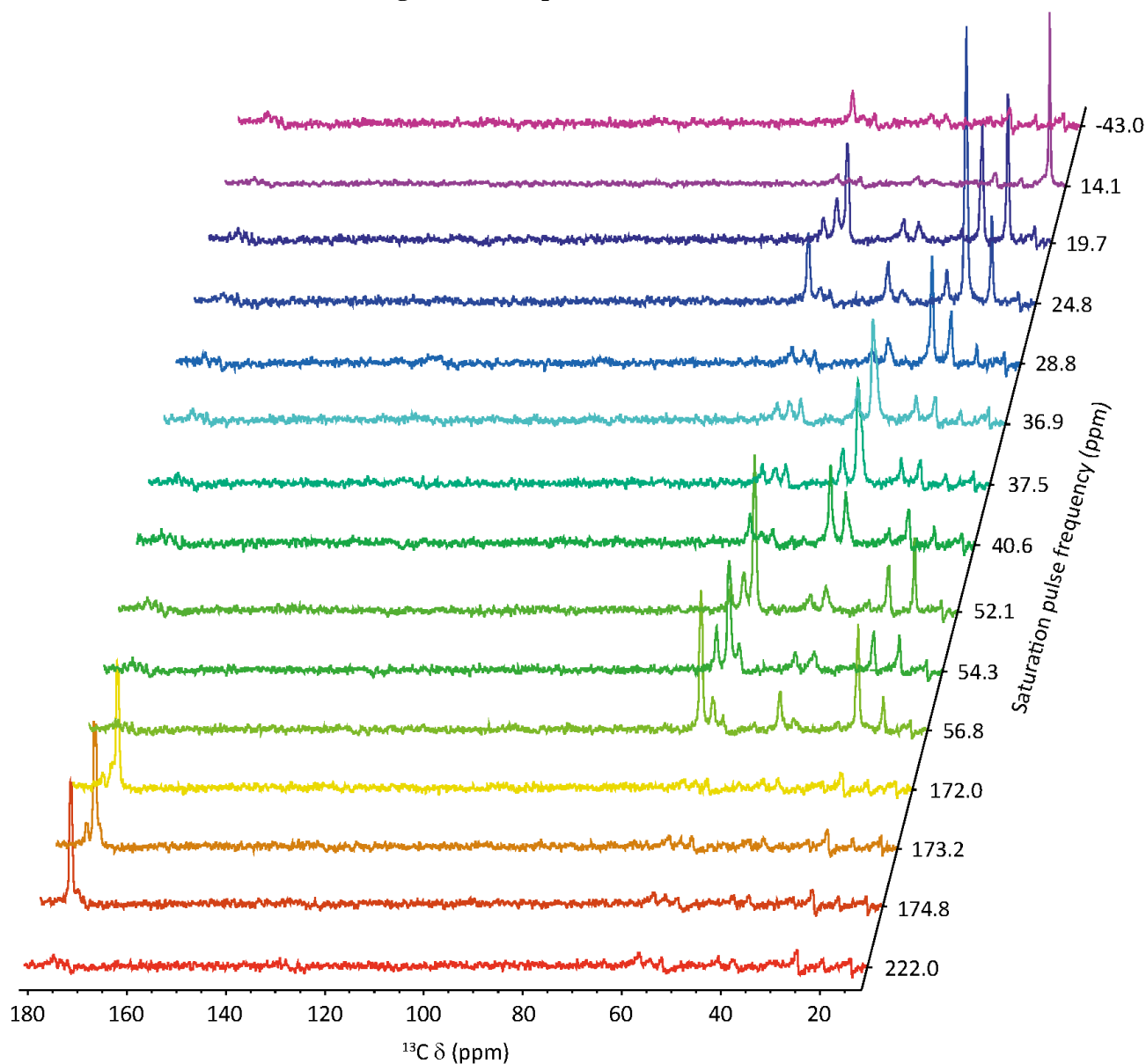
Figure S2. Alternative method of visualising the difference 2D ^{13}C SEXY spectrum taken during optimisation at a pulse power of 65 Hz and saturation duration of 0.30 s. This method of spectral reconstruction allows saturation transfer to be visualised without the presence of streaks and highlighted clearly the sample heating issue.

Proton-driven spin diffusion
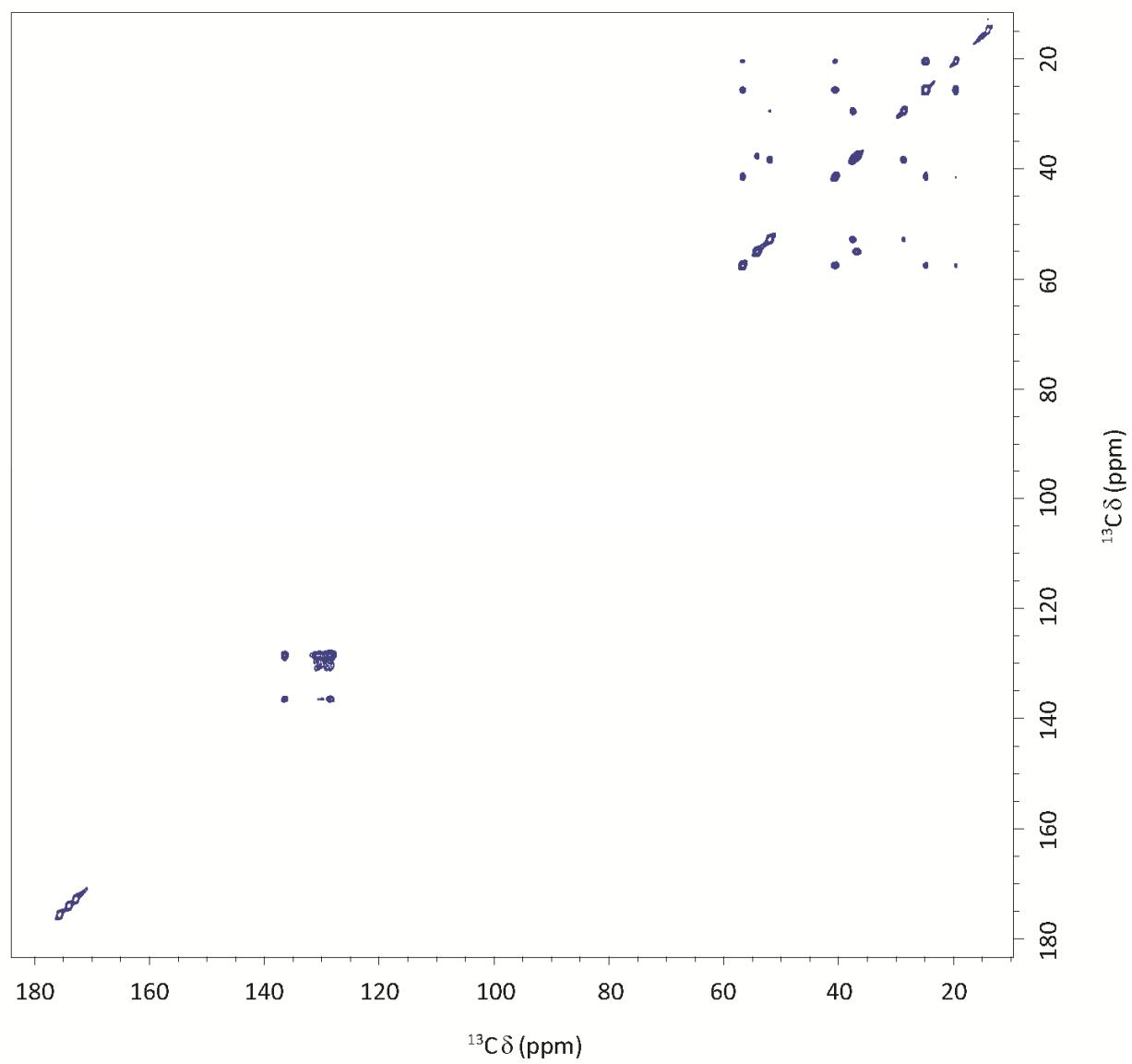
Figure S2. Full ¹³C-¹³C PDSD spectrum of MLF (0.3 s mixing time).

T_1 relaxation data

Table S1. T_1 relaxation data at fast spinning frequencies (60 kHz). All values below -0.2 s are highlighted in red.

| | Fast spinning frequencies (60 kHz) | | | |
Saturation frequency (ppm)	Peak (ppm)	T_1 relax (s)	Difference in T_1 between saturated and unsaturated (s)	Normalised T_1
no pulse	56.8	3.647		
no pulse	54.3	4.548		
no pulse	53.2	2.612		
no pulse	40.7	1.331		
no pulse	37.6	0.849		
no pulse	37.2	1.402		
no pulse	28.8	0.808		
no pulse	24.9	1.188		
no pulse	19.7	0.984		
no pulse	14.1	2.643		
636.2	56.8	3.016		
636.2	54.3	3.944		
636.2	53.2	3.568		
636.2	40.7	1.294		
636.2	37.6	0.788		
636.2	37.2	1.204		
636.2	28.8	0.794		
636.2	24.9	0.94		
636.2	19.7	1.113		
636.2	14.1	1.463		
174.8	175	0.197		
174.8	173.5	8.924		
174.8	172.2	13.482		
174.8	56.8	3.727	-0.686	-0.226
174.8	54.3	4.889	0.252	0.049

174.8	53.2	3.122	-0.153	-0.052
174.8	40.7	1.423	0.037	0.025
174.8	37.6	0.874	0.011	0.012
174.8	37.2	1.259	0.123	0.089
174.8	28.8	0.778	0.044	0.054
174.8	24.9	1.03	0.054	0.050
174.8	19.7	1	0.221	0.181
174.8	14.1	1.881	0.382	0.169
173.1	175	15.38		
173.1	173.5	0.311		
173.1	172.2	14.617		
173.1	56.8	3.233	-0.192	-0.063
173.1	54.3	5.384	-0.243	-0.047
173.1	53.2	3.033	-0.064	-0.022
173.1	40.7	1.391	0.069	0.047
173.1	37.6	0.831	0.054	0.061
173.1	37.2	1.387	-0.005	-0.004
173.1	28.8	0.896	-0.074	-0.090
173.1	24.9	1.081	0.003	0.003
173.1	19.7	1.059	0.162	0.133
173.1	14.1	2.567	-0.304	-0.134
171.8	175	11.733		
171.8	173.5	45.478		
171.8	172.2	0.237		
171.8	56.8	3.893	-0.852	-0.280
171.8	54.3	5.111	0.03	0.006
171.8	53.2	3.016	-0.047	-0.016
171.8	40.7	1.306	0.154	0.105
171.8	37.6	0.85	0.035	0.040
171.8	37.2	1.367	0.015	0.011
171.8	28.8	0.829	-0.007	-0.009
171.8	24.9	1.11	-0.026	-0.024

171.8	19.7	1.081	0.14	0.115
171.8	14.1	2.403	-0.14	-0.062
135.6	56.8	3.405	-0.364	-0.120
135.6	54.3	4.276	0.865	0.168
135.6	53.2	2.976	-0.007	-0.002
135.6	40.7	1.419	0.041	0.028
135.6	37.6	0.904	-0.019	-0.021
135.6	37.2	1.512	-0.13	-0.094
135.6	28.8	0.877	-0.055	-0.067
135.6	24.9	1.104	-0.02	-0.018
135.6	19.7	1.145	0.076	0.062
135.6	14.1	2.522	-0.259	-0.114
129.8	56.8	6.219	-3.178	-1.045
129.8	54.3	3.646	1.495	0.291
129.8	53.2	2.659	0.31	0.104
129.8	40.7	1.307	0.153	0.105
129.8	37.6	0.248	0.637	0.720
129.8	37.2	1.214	0.168	0.122
129.8	28.8	0.722	0.1	0.122
129.8	24.9	1.035	0.049	0.045
129.8	19.7	1.209	0.012	0.010
129.8	14.1	2.035	0.228	0.101
127.6	56.8	3.621	-0.58	-0.191
127.6	54.3	4.125	1.016	0.198
127.6	53.2	3.301	-0.332	-0.112
127.6	40.7	1.285	0.175	0.120
127.6	37.6	0.968	-0.083	-0.094
127.6	37.2	1.605	-0.223	-0.161
127.6	28.8	0.894	-0.072	-0.088
127.6	24.9	1.184	-0.1	-0.092
127.6	19.7	1.3	-0.079	-0.065
127.6	14.1	2.486	-0.223	-0.099

89.5	56.8	3.75	-0.709	-0.233
89.5	54.3	5.37	-0.229	-0.045
89.5	53.2	3.078	-0.109	-0.037
89.5	40.7	1.287	0.173	0.118
89.5	37.6	0.948	-0.063	-0.071
89.5	37.2	1.413	-0.031	-0.022
89.5	28.8	0.799	0.023	0.028
89.5	24.9	1.046	0.038	0.035
89.5	19.7	1.082	0.139	0.114
89.5	14.1	2.393	-0.13	-0.057
56.6	56.8	0.645	2.396	0.788
56.6	54.3	16281	-16275.859	-3166
56.6	53.2	6723.5	-6720.531	-2264
56.6	40.7	1.107	0.353	0.242
56.6	37.6	0.574	0.311	0.351
56.6	37.2	0.986	0.396	0.287
56.6	28.8	0.587	0.235	0.286
56.6	24.9	0.812	0.272	0.251
56.6	19.7	1.218	0.003	0.002
56.6	14.1	0.35	2.691	0.885
54.2	56.8	2.675	0.366	0.120
54.2	54.3	0.65	4.491	0.874
54.2	53.2	2.388	0.581	0.196
54.2	40.7	1.101	0.359	0.246
54.2	37.6	0.242	0.643	0.727
54.2	37.2	0.814	0.568	0.411
54.2	28.8	0.755	0.067	0.082
54.2	24.9	1.057	0.027	0.025
54.2	19.7	0.573	0.648	0.531
54.2	14.1	1.984	0.279	0.123
51.8	56.8	2.901	0.14	0.046
51.8	54.3	3.892	1.249	0.243

51.8	53.2	0.574	2.395	0.807
51.8	40.7	1.416	0.044	0.030
51.8	37.6	0.772	0.113	0.128
51.8	37.2	1.268	0.114	0.082
51.8	28.8	0.77	0.052	0.063
51.8	24.9	1.082	0.002	0.002
51.8	19.7	1.241	-0.02	-0.016
51.8	14.1	2.798	-0.535	-0.236
40.4	56.8	2.676	0.365	0.120
40.4	54.3	4.382	0.759	0.148
40.4	53.2	2.955	0.014	0.005
40.4	40.7	0.929	0.531	0.364
40.4	37.6	0.765	0.12	0.136
40.4	37.2	1.163	0.219	0.158
40.4	28.8	0.792	0.03	0.036
40.4	24.9	1.069	0.015	0.014
40.4	19.7	1.045	0.176	0.144
40.4	14.1	2.152	0.111	0.049
37.7	56.8	3.14	-0.099	-0.033
37.7	54.3	3.302	1.839	0.358
37.7	53.2	2.788	0.181	0.061
37.7	40.7	0.959	0.501	0.343
37.7	37.6	0.527	0.358	0.405
37.7	37.2	0.847	0.535	0.387
37.7	28.8	0.736	0.086	0.105
37.7	24.9	1.006	0.078	0.072
37.7	19.7	1.386	-0.165	-0.135
37.7	14.1	2.663	-0.4	-0.177
36.8	56.8	3.184	-0.143	-0.047
36.8	54.3	3.321	1.82	0.354
36.8	53.2	2.871	0.098	0.033
36.8	40.7	1.391	0.069	0.047

36.8	37.6	0.644	0.241	0.272
36.8	37.2	0.848	0.534	0.386
36.8	28.8	0.746	0.076	0.092
36.8	24.9	1.11	-0.026	-0.024
36.8	19.7	1.116	0.105	0.086
36.8	14.1	1.69	0.573	0.253
28.2	56.8	3.109	-0.068	-0.022
28.2	54.3	3.963	1.178	0.229
28.2	53.2	3.039	-0.07	-0.024
28.2	40.7	1.345	0.115	0.079
28.2	37.6	0.778	0.107	0.121
28.2	37.2	1.331	0.051	0.037
28.2	28.8	0.463	0.359	0.437
28.2	24.9	1.09	-0.006	-0.006
28.2	19.7	1.095	0.126	0.103
28.2	14.1	2.521	-0.258	-0.114
24.8	56.8	3.162	-0.121	-0.040
24.8	54.3	3.585	1.556	0.303
24.8	53.2	3.327	-0.358	-0.121
24.8	40.7	0.995	0.465	0.318
24.8	37.6	0.86	0.025	0.028
24.8	37.2	1.381	0.001	0.001
24.8	28.8	0.8	0.022	0.027
24.8	24.9	0.505	0.579	0.534
24.8	19.7	0.678	0.543	0.445
24.8	14.1	2.952	-0.689	-0.304
19.4	56.8	2.989	0.052	0.017
19.4	54.3	4.983	0.158	0.031
19.4	53.2	3.079	-0.11	-0.037
19.4	40.7	1.226	0.234	0.160
19.4	37.6	0.902	-0.017	-0.019
19.4	37.2	1.338	0.044	0.032

19.4	28.8	0.923	-0.101	-0.123
19.4	24.9	0.79	0.294	0.271
19.4	19.7	0.602	0.619	0.507
19.4	14.1	2.16	0.103	0.046
13.7	56.8	3.563	-0.522	-0.172
13.7	54.3	3.939	1.202	0.234
13.7	53.2	3.218	-0.249	-0.084
13.7	40.7	1.165	0.295	0.202
13.7	37.6	1.004	-0.119	-0.134
13.7	37.2	1.581	-0.199	-0.144
13.7	28.8	0.84	-0.018	-0.022
13.7	24.9	1.12	-0.036	-0.033
13.7	19.7	1.264	-0.043	-0.035
13.7	14.1	0.45	1.813	0.801
-440.6984758	56.8	3.041		
-440.6984758	54.3	5.141		
-440.6984758	53.2	2.969		
-440.6984758	40.7	1.46		
-440.6984758	37.6	0.885		
-440.6984758	37.2	1.382		
-440.6984758	28.8	0.822		
-440.6984758	24.9	1.084		
-440.6984758	19.7	1.221		
-440.6984758	14.1	2.263		

Table S2. T_1 relaxation data at slow spinning frequencies (13.3 kHz).

		Slow spinning frequency (13.3 kHz)		
Saturation frequency (ppm)	Peak (ppm)	T_1 relax points removed (s)	Difference in T_1 between saturated and unsaturated (s)	Normalis ed T_1
no pulse	175	1.783		
no pulse	173.5	3.44		
no pulse	172.2	1.691		
no pulse	135.7	5.918		
no pulse	131	3.809		
no pulse	127.9	4.685		
no pulse	56.8	1.295		
no pulse	54.3	4.996		
no pulse	53.2	1.049		
no pulse	40.7	1.09		
no pulse	37.6	0.954		
no pulse	37.2	2.578		
no pulse	28.8	0.5		
no pulse	24.9	0.759		
no pulse	19.7	0.701		
no pulse	14.1	2.039		
1149.8	175	1.736		
1149.8	173.5	5.746		
1149.8	172.2	1.723		
1149.8	135.7	5.4		
1149.8	131	4.749		
1149.8	127.9	3.857		
1149.8	56.8	1.358		
1149.8	54.3	5.614		
1149.8	53.2	1.158		
1149.8	40.7	1.213		

1149.8	37.6	1.01		
1149.8	37.2	2.362		
1149.8	28.8	0.577		
1149.8	24.9	0.791		
1149.8	19.7	0.719		
1149.8	14.1	1.588		
174.9	175	0.0002	1.736	1.000
174.9	173.5	0.011	5.735	0.998
174.9	172.2	0.022	1.701	0.987
174.9	135.7	0.198	5.202	0.963
174.9	131	0.235	4.514	0.951
174.9	127.9	0.24	3.617	0.938
174.9	56.8	0.119	1.239	0.912
174.9	54.3	0.1	5.514	0.982
174.9	53.2	0.17	0.988	0.853
174.9	40.7	0.158	1.055	0.870
174.9	37.6	0.17	0.84	0.832
174.9	37.2	0.155	2.207	0.934
174.9	28.8	0.179	0.398	0.690
174.9	24.9	0.191	0.6	0.759
174.9	19.7	0.195	0.524	0.729
174.9	14.1	0.604	0.984	0.620
173.3	175	0.038	1.698	0.978
173.3	173.5	0.009	5.737	0.998
173.3	172.2	0.004	1.719	0.998
173.3	135.7	0.231	5.169	0.957
173.3	131	0.246	4.503	0.948
173.3	127.9	0.226	3.631	0.941
173.3	56.8	0.141	1.217	0.896
173.3	54.3	0.102	5.512	0.982
173.3	53.2	0.146	1.012	0.874
173.3	40.7	0.175	1.038	0.856

173.3	37.6	0.161	0.849	0.841
173.3	37.2	0.15	2.212	0.936
173.3	28.8	0.165	0.412	0.714
173.3	24.9	0.204	0.587	0.742
173.3	19.7	0.215	0.504	0.701
173.3	14.1	0.611	0.977	0.615
172.0	175	0.12	1.616	0.931
172.0	173.5	0.118	5.628	0.979
172.0	172.2	0.134	1.589	0.922
172.0	135.7	0.244	5.156	0.955
172.0	131	0.262	4.487	0.945
172.0	127.9	0.237	3.62	0.939
172.0	56.8	0.013	1.345	0.990
172.0	54.3	0.011	5.603	0.998
172.0	53.2	0.03	1.128	0.974
172.0	40.7	0.045	1.168	0.963
172.0	37.6	0.052	0.958	0.949
172.0	37.2	0.029	2.333	0.988
172.0	28.8	0.067	0.51	0.884
172.0	24.9	0.104	0.687	0.869
172.0	19.7	0.127	0.592	0.823
172.0	14.1	0.497	1.091	0.687
56.7	175	0.126	1.61	0.927
56.7	173.5	0.11	5.636	0.981
56.7	172.2	0.128	1.595	0.926
56.7	135.7	0.156	5.244	0.971
56.7	131	0.158	4.591	0.967
56.7	127.9	0.155	3.702	0.960
56.7	56.8	0.025	1.333	0.982
56.7	54.3	0.014	5.6	0.998
56.7	53.2	0.019	1.139	0.984
56.7	40.7	0.06	1.153	0.951

56.7	37.6	0.045	0.965	0.955
56.7	37.2	0.051	2.311	0.978
56.7	28.8	0.062	0.515	0.893
56.7	24.9	0.0108	0.780	0.986
56.7	19.7	0.122	0.597	0.830
56.7	14.1	0.485	1.103	0.695
54.3	175	0.14	1.596	0.919
54.3	173.5	0.116	5.63	0.980
54.3	172.2	0.126	1.597	0.927
54.3	135.7	0.13	5.27	0.976
54.3	131	0.136	4.613	0.971
54.3	127.9	0.129	3.728	0.967
54.3	56.8	0.046	1.312	0.966
54.3	54.3	0.02	5.594	0.996
54.3	53.2	0.013	1.145	0.989
54.3	40.7	0.067	1.146	0.945
54.3	37.6	0.037	0.973	0.963
54.3	37.2	0.049	2.313	0.979
54.3	28.8	0.053	0.524	0.908
54.3	24.9	0.112	0.679	0.858
54.3	19.7	0.125	0.594	0.826
54.3	14.1	0.485	1.103	0.695
52.0	175	0.14	1.596	0.919
52.0	173.5	0.116	5.63	0.980
52.0	172.2	0.126	1.597	0.927
52.0	135.7	0.108	5.292	0.980
52.0	131	0.085	4.664	0.982
52.0	127.9	0.079	3.778	0.980
52.0	56.8	0.046	1.312	0.966
52.0	54.3	0.02	5.594	0.996
52.0	53.2	0.013	1.145	0.989
52.0	40.7	0.067	1.146	0.945

52.0	37.6	0.038	0.972	0.962
52.0	37.2	0.049	2.313	0.979
52.0	28.8	0.053	0.524	0.908
52.0	24.9	0.113	0.678	0.857
52.0	19.7	0.125	0.594	0.826
52.0	14.1	0.484	1.104	0.695
40.7	175	0.185	1.551	0.893
40.7	173.5	0.162	5.584	0.972
40.7	172.2	0.177	1.546	0.897
40.7	135.7	0.105	5.295	0.981
40.7	131	0.08	4.669	0.983
40.7	127.9	0.073	3.784	0.981
40.7	56.8	0.086	1.272	0.937
40.7	54.3	0.073	5.541	0.987
40.7	53.2	0.054	1.104	0.953
40.7	40.7	0.057	1.156	0.953
40.7	37.6	0.027	0.983	0.973
40.7	37.2	0.047	2.315	0.980
40.7	28.8	0.034	0.543	0.941
40.7	24.9	0.092	0.699	0.884
40.7	19.7	0.108	0.611	0.850
40.7	14.1	0.447	1.141	0.719
37.8	175	0.185	1.551	0.893
37.8	173.5	0.16	5.586	0.972
37.8	172.2	0.176	1.547	0.898
37.8	135.7	0.103	5.297	0.981
37.8	131	0.08	4.669	0.983
37.8	127.9	0.73	3.127	0.811
37.8	56.8	0.091	1.267	0.933
37.8	54.3	0.072	5.542	0.987
37.8	53.2	0.055	1.103	0.953
37.8	40.7	0.059	1.154	0.951

37.8	37.6	0.022	0.988	0.978
37.8	37.2	0.035	2.327	0.985
37.8	28.8	0.026	0.551	0.955
37.8	24.9	0.082	0.709	0.896
37.8	19.7	0.099	0.62	0.862
37.8	14.1	0.426	1.162	0.732
36.8	175	0.187	1.549	0.892
36.8	173.5	0.161	5.585	0.972
36.8	172.2	0.174	1.549	0.899
36.8	135.7	0.102	5.298	0.981
36.8	131	0.083	4.666	0.983
36.8	127.9	0.08	3.777	0.979
36.8	56.8	0.095	1.263	0.930
36.8	54.3	0.071	5.543	0.987
36.8	53.2	0.054	1.104	0.953
36.8	40.7	0.06	1.153	0.951
36.8	37.6	0.023	0.987	0.977
36.8	37.2	0.037	2.325	0.984
36.8	28.8	0.025	0.552	0.957
36.8	24.9	0.081	0.71	0.898
36.8	19.7	0.097	0.622	0.865
36.8	14.1	0.419	1.169	0.736
28.5	175	0.181	1.555	0.896
28.5	173.5	0.229	5.517	0.960
28.5	172.2	0.192	1.531	0.889
28.5	135.7	0.257	5.143	0.952
28.5	131	0.24	4.509	0.949
28.5	127.9	0.225	3.632	0.942
28.5	56.8	0.091	1.267	0.933
28.5	54.3	0.145	5.469	0.974
28.5	53.2	0.079	1.079	0.932
28.5	40.7	0.056	1.157	0.954

28.5	37.6	0.044	0.966	0.956
28.5	37.2	0.104	2.258	0.956
28.5	28.8	0.014	0.563	0.976
28.5	24.9	0.028	0.763	0.965
28.5	19.7	0.047	0.672	0.935
28.5	14.1	0.35	1.238	0.780
24.8	175	0.179	1.557	0.897
24.8	173.5	0.269	5.477	0.953
24.8	172.2	0.204	1.519	0.882
24.8	135.7	0.349	5.051	0.935
24.8	131	0.307	4.442	0.935
24.8	127.9	0.296	3.561	0.923
24.8	56.8	0.073	1.285	0.946
24.8	54.3	0.185	5.429	0.967
24.8	53.2	0.098	1.06	0.915
24.8	40.7	0.042	1.171	0.965
24.8	37.6	0.062	0.948	0.939
24.8	37.2	0.148	2.214	0.937
24.8	28.8	0.023	0.554	0.960
24.8	24.9	0.007	0.784	0.991
24.8	19.7	0.021	0.698	0.971
24.8	14.1	0.314	1.274	0.802
19.5	175	0.21	1.526	0.879
19.5	173.5	0.332	5.414	0.942
19.5	172.2	0.264	1.459	0.847
19.5	135.7	0.38	5.02	0.930
19.5	131	0.396	4.353	0.917
19.5	127.9	0.407	3.45	0.894
19.5	56.8	0.095	1.263	0.930
19.5	54.3	0.238	5.376	0.958
19.5	53.2	0.144	1.014	0.876
19.5	40.7	0.061	1.152	0.950

19.5	37.6	0.103	0.907	0.898
19.5	37.2	0.209	2.153	0.912
19.5	28.8	0.054	0.523	0.906
19.5	24.9	0.025	0.766	0.968
19.5	19.7	0.004	0.715	0.994
19.5	14.1	0.14	1.448	0.912
13.9	175	0.296	1.44	0.829
13.9	173.5	0.442	5.304	0.923
13.9	172.2	0.322	1.401	0.813
13.9	135.7	0.561	4.839	0.896
13.9	131	0.557	4.192	0.883
13.9	127.9	0.547	3.31	0.858
13.9	56.8	0.191	1.167	0.859
13.9	54.3	0.341	5.273	0.939
13.9	53.2	0.211	0.947	0.818
13.9	40.7	0.151	1.062	0.876
13.9	37.6	0.161	0.849	0.841
13.9	37.2	0.296	2.066	0.875
13.9	28.8	0.099	0.478	0.828
13.9	24.9	0.105	0.686	0.867
13.9	19.7	0.083	0.636	0.885
13.9	14.1	0.0002	1.588	1.000
-970.9	135.7	1.857		
-970.9	131	5.856		
-970.9	127.9	1.782		
-970.9	135.7	4.49		
-970.9	131	4.438		
-970.9	127.9	4.614		
-970.9	56.8	1.337		
-970.9	54.3	3.765		
-970.9	53.2	1.131		
-970.9	40.7	1.193		

-970.9	37.6	1.097
-970.9	37.2	3.1
-970.9	28.8	0.567
-970.9	24.9	0.797
-970.9	19.7	0.753
-970.9	14.1	1.603